A computer algorithm for determining the tensile strength of float glass

M. Overend* & K. Zammit

Department of Engineering, University of Cambridge, CB2 1PZ, UK

Abstract

The extrinsic tensile strength of glass can be determined explicitly if the characteristics of the critical surface flaw are known, or stochastically if the critical flaw characteristics are unknown. This paper makes contributions to both these approaches. Firstly it presents a unified model for determining the strength of glass explicitly, by accounting for both the inert strength limit and the sub-critical crack growth threshold. Secondly, it describes and illustrates the use of a numerical algorithm, based on the stochastic approach, that computes the characteristic tensile strength of float glass by piecewise summation of the surface stresses. The experimental validation and sensitivity analysis reported in this paper show that the proposed computer algorithm provides an accurate and efficient means of determining the characteristic strength of float glass. The algorithm is particularly useful for annealed and thermally treated float glass used in the construction industry.

Keywords: Glass strength; Glass design; Glass failure prediction; Glass failure probability.

*Corresponding author Tel: +44 (0)1223 332659
Fax: +44 (0)1223 332662
Email: mo318@cam.ac.uk

1. Introduction

Soda-lime-silica glass is a ubiquitous material in buildings. It is traditionally used as an infill rectangular plate in the building fabric, where the glass is simply-supported along two or four edges by timber or metal sub-frames. Simple rules-of-thumb and glass thickness selection charts are sufficiently accurate for sizing such glass plates, but these methods are limited to simple boundary conditions and uniform pressures. The novel uses of glass such as non-rectangular glass plates, unconventional boundary conditions (Fig. 1) and the use of glass in primary load-bearing elements (Fig. 2) are fuelling a need for more accurate and more widely applicable design methods.

Figure 1, Figure 2

Glass is an isotropic, almost perfectly elastic, material that exhibits brittle fracture. The intrinsic (i.e. flawless) tensile strength, based on interatomic force calculations, is 32GPa [1]. However, the extrinsic tensile strength of annealed glass, i.e. the strength of glass in practice, is less than 100MPa.

This discrepancy arises from stress-raising microscopic flaws on the glass surface (Griffith flaws) that are induced during the manufacturing and handling of glass, and accumulate from weathering during its service life. The surface of weathered float glass generally contains a large number of these flaws (Fig. 3). The flaws visible in this micrograph of a 20-year old glass window include linear scratches probably caused during the handling / installation of the glass, and pitting attributed to impact damage from flying debris and prolonged biological attack on the glass surface. Interestingly the biological attack seems to be most severe close to the mechanical damage probably indicating that biological growth is more likely to occur in or around pre-existing flaws on the surface.

Figure 3

When the tensile stress at the tip of a narrow elliptical flaw (henceforth referred to as a crack) exceeds the inter-molecular bond strength, the crack grows rapidly at speeds of 1.5mm/μs to 2.5mm/μs, which

is perceived as fast fracture [2]. Irwin [3] described the stress intensity at the crack tip in terms of the stress intensity factor, *K*, which for mode I loading is:

$$K_I = Y\sigma\sqrt{\pi a} \tag{1}$$

Where σ is the tensile stress normal to the crack, a is the crack depth or half the crack length and Y is a geometry factor that accounts for the crack geometry and the proximity of the specimen boundaries (Y = 0.713 for half penny shaped cracks and Y = 1.12 for straight front plane edge cracks in a semi-infinite solid). Fast fracture occurs when the stress intensity factor exceeds the plane strain fracture toughness K_{IC} , that ranges from 0.72 to 0.82 MPa $m^{1/2}$ for soda lime silica glass. In the absence of more detailed geometrical characteristics of real-world surface cracks, values of K_{IC} = 0.75 MPa $m^{1/2}$ and Y = 1.12 will be used in this paper, as recommended by Haldimann *et al.* [4]. Substituting $2a$ = 100μm for moderately weathered glass and $2a$ = 2mm, for macroscopic chips into Eq. (1) gives extrinsic strengths of σ=37.8 MPa and σ=8.4 MPa respectively, which are typical of the extrinsic strengths encountered in practice.

However, Griffith theory and the analogous stress intensity approach proposed by Irwin (Eq. 1) ignore other influences such as the effects of humidity which, if present, causes a crack to grow sub-critically until it reaches a critical size that triggers fast fracture. Eq.(1) is therefore only valid in inert conditions (e.g. a vacuum). Sub-critical crack growth (also known as stress corrosion or static fatigue) is a function of several parameters, in particular the condition of the surface, the stress history (intensity and duration), the residual stresses acting across the crack and the environmental conditions [4].

This phenomenon is central to the lifetime prediction of ceramics and has been researched extensively since the 1960's. A detailed account of the vast number of publications in this field is beyond the scope of this paper and can be found elsewhere [5],[6],[7],[8]. A brief overview of the salient research is provided here.

The problem of sub-critical crack growth has been studied since 1899 [9], but the first comprehensive study was undertaken by Mould and Southwick [10],[11] who showed that the time to failure was a function of the applied stress. In a seminal paper, Wiederhorn [12] measured crack velocities as a function of stress intensity with varying quantities of H_2O, thereby showing that the crack growth curve could be divided in to three regions (Fig A1). Region I represents the reaction-rate crack growth governed by the chemical reaction between glass and water in the environment. Region II is governed by the rate of transport of water to the crack tip; in region III, the crack growth is independent of water in the environment. A qualitative molecular model describing sub-critical crack growth for water interacting with stressed silicates, i.e. regions I and II, is described by Michalske and Freiman [13].

Evans and Wiederhorn [14] showed that the logarithmic v-K_I plot in region I is linear and for constant environmental conditions may be expressed empirically as:

$$v = A K_I^n. \quad (2)$$

which may also be expressed as:

$$da/dt = v = v_0 (K_I / K_{IC})^n \quad (3)$$

Where the crack velocity parameters A, v_0 and n depend on the material, the temperature and the environment (v_0=6mm/s and n=16 are conservative estimates of in-service conditions of float glass in buildings, and v_0=30mm/s and n=16 are representative of glass permanently immersed in water [15]).

This agrees with the theory of Charles and Hillig [16] who described the relationship between the chemically assisted sub-critical crack velocity and the applied stress in terms of the activation energy. Further agreement that region I is governed by chemical reaction is provided by Wiederhorn and Johnson [17] and Wiederhorn and Bolz [18] who showed that the rate of crack propagation increases with pH value and temperature respectively.

Crack growth appears to approach a threshold at low velocities, below which crack growth arrests. This represents a fourth region in the v-K_I relationship defined by the sub-critical crack growth threshold K_{TH}, (Fig A1). Wiederhorn and Boltz [18] and Wilkins and Dutton [19] show evidence of a sub-critical crack growth threshold in soda-lime glass. The reasons for this threshold are yet to be fully explained, but a plausible hypothesis is that alkalis are leached out of the glass and change the chemical composition of the crack tip [20],[21]. Munz and Fett [7] also claimed that a threshold can be detected in glass, and they developed a mechanics-inspired spring model of the crack to show that at sufficiently low magnitudes of externally applied load there are no additional states of equilibrium, and the crack cannot grow. They used this energy approach to plot modified v-K_I relationships that account for the subcritical crack growth threshold and they reported good agreement with the experimental data reported by Evans [22] for K_{TH}/K_{IC} = 0.23 and n=14. Haldimann [15] recommended a sub-critical crack growth limit K_{TH}= 0.25 MPa m$^{1/2}$ for most applications, and K_{TH} = 0.2 MPa m$^{1/2}$ for high levels of humidity.

A number of studies have implemented this research on sub-critical crack growth to the lifetime prediction of float glass intended for architectural applications [23] to [29]. An overview of this research is available in Haldimann *et al.* [4].

NASGRO [30] is a stand-alone fracture mechanics and fatigue crack growth analysis software package. NASGRO is used to assess stress intensity and crack growth of single cracks under a sustained static stress. Sub-critical crack growth is treated in detail, including a formulation that simultaneously accounts for the crack growth threshold and the critical stress. NASGRO can also compute stress intensity factors for complex crack configurations, critical crack sizes and crack initiation in components. The implementation of the sustained stress analysis for glass-like materials is provided by the NASGLS module. This is limited to a Paris-type model as shown in Eq. (3) thereby ignoring the presence of the inert strength limit and the sub-critical crack growth threshold.

Another notable development in this field is the work of Haldimann [15] who adopted a similar approach to Munz and Fett [7] to solve the ordinary differential equation for crack growth by substituting Eq.(1) into Eq.(3). This yields an expression for the uniform failure stress σ_f of a surface crack in annealed glass as a function of the stress duration and the crack geometry:

$$\sigma_f = \left\{ \left[\frac{1}{t_f} \frac{2}{(n-2)\, v_0\, K_{IC}^{-n} \left(Y\sqrt{\pi}\right)^n\, a_i^{(n-2)/2}} \right] \left[1 - \left(\frac{a_i}{a_f} \right)^{(n-2)/2} \right] \right\}^{1/n} \tag{4}$$

Where t_f represents the time to failure of a crack with the initial crack size (i.e. crack depth or half the crack length) a_i and a_f represents the size of the crack at failure. In Eq. (4) the failure stress of annealed glass is asymptotic to the inert strength at very short durations i.e. as $t_f \rightarrow 0$, $\sigma_f \rightarrow K_{IC} / (Y(\pi a)^{½})$, but it converges to zero for long durations, thereby failing to account for the sub-critical crack growth threshold K_{TH},. In fact, despite several reports about the existence of a sub-critical crack growth threshold in soda lime glass, none of the existing lifetime prediction models reviewed provide a unified model that accounts for both the inert strength limit and the sub-critical crack growth threshold.

In practice the location and orientation of the surface cracks are generally unknown. The current generation of glass design guidelines therefore adopt a stochastic approach [31],[32],[33]. Behr *et al.* [34] showed that the variability of glass strength is best described by a 2-parameter Weibull probability distribution function such that:

$$P_f = 1 - \exp\left(-kA\sigma^m\right) \tag{5}$$

Where m and k are the interdependent Weibull parameters determined from load-testing of nominally identical glass specimens and σ is the net crack-opening stress at the origin of failure, i.e. $\sigma = (\sigma_f + f_{rk})$. Where σ_f is the load-induced surface stress and f_{rk} is the residual surface stresses caused by the

thermal or chemical treatment process. Residual stresses are generally compressive and therefore have a negative sign.

The characteristic tensile strength of glass (i.e. the tensile strength for a given probability of failure) can therefore be determined from Eq. (5). This is valid for the particular stress state and stress history of the test specimens, but can be converted into a characteristic equibiaxial tensile strength $f_{gk,\,t0.\,A0}$ for an arbitrary reference stress duration t_0 over a reference area A_0. [35].

In most real-world applications, the principal surface stress $\sigma_1(x,y,t)$ varies across the glass surface (x,y) and time (t) as a function of boundary conditions and transient loading. Furthermore, in thermally treated glass, the surface pre-compression is distorted close to free edges and holes in the glass., therefore, $f_{rk}\,(x,y)$ is a function of the proximity of free edges as well as quality control of the tempering process [36],[37]. Overend *et al.* [28] describe how the contributions of all the time-resolved surface tensile stresses resulting from a design sceanrio can be converted into an equivalent uniform equibiaxial stress $\sigma_{p,\,t0.\,A0}$ applied for a stress duration $(t_0 - t_r)$ over area A_0:

$$\sigma_{p,t0,A0} = \left\{ \frac{1}{A_0} \int_{area} \left[\frac{1}{(t_0 - t_r)} \int_{t_r}^{t_d} \left[c_b \sigma_1(x,y,t) + f_{rk}(x.y) \right]^n dt \right]^{m/n} dA \right\}^{1/m} \tag{6}$$

where c_b is a biaxial stress correction factor that accounts for the effect of unequal biaxial stresses on the mode *I* crack opening stress [24] and $(t_0 - t_r)$ is the duration for which the applied surface stress $\sigma_1(x,y,t)$ exceeds the magnitude of $f_{rk}\,(x,y)$ and t_d is duration of the design scenario. Eq. (6) therefore represents the equivalent uniform equibiaxial stress net of pre-compression.

The equivalent uniform equibiaxial stress $\sigma_{p,\,t0.\,A0}$ can be compared directly to the characteristic equibiaxial strength of glass $f_{gk,\,t0.\,A0}$ to ensure that:

$$f_{gk,t0,A0} \geq \sigma_{p,t0,A0} \tag{7}$$

This approach implies that sub-critical crack growth commences when $[\sigma_I(x,y,t) + f_{rk}(x,y)] = 0$, thereby ignoring the presence of a threshold. Another disadvantage of the stochastic approach is the computation of Eq. (6) that involves the subdivision of the glass surface into areas, *dA*, and time steps, *dt*, with sufficiently small stress gradients, followed by the piecewise summation of the time-resolved surface stresses. This is laborious and unattractive for manual computation. An automated approach for a simple version of Eq. (6), based on the work of Sedlacek et. al. [25], was first implemented in SJ MEPLA v2, a specialist glass finite element software, but has since been excluded from more recent versions of the software [38]. Both Overend [39] and Haldimann [15] propose automated processes for computing Eq. (6), but the former ignores the presence of the inert strength limit and the sub-critical crack growth threshold while the latter ignores the crack growth threshold.

Ceramics Analysis and Reliability Evaluation of Structures (CARES) [40] is a post-processor to commercial Finite Element Analysis (FEA) software using a custom neutral file format. CARES adopts a stochastic approach to both volume and surface flaws in ceramics and accounts for the effects of distributed flaws by characterising ceramic material strength with a Weibull distribution. The overall component reliability is computed as the product of all the calculated element survival probabilities of each element in the finite element model of the component [41]. Multi-axial stress states are assessed using Batdorf's Theory [42] which is extended to account for sub-critical crack growth using the Paris-type power law shown in Eq (2). This approach is very similar to the lifetime prediction model of Haldimann *et al.* [4]. In addition, CARES also considers crack growth due dynamic fatigue as a result of cyclic loading. The software has been applied to soda lime glass, where static and dynamic fatigue parameters have been evaluated through coaxial double ring (CDR) tests [43]. However CARES does not consider the sub-critical crack growth threshold, the inert strength limit or the presence of surface pre-compression.

This paper builds on the above-mentioned research and addresses the principal limitations of the explicit and stochastic approaches, particularly in their implementation to float glass used in the construction industry by:

(a) Extending the glass strength model to include both an upper bound to the strength of glass imposed by the inert strength limit and a lower bound governed by the subcritical crack growth threshold.

(b) Developing a computer algorithm that performs a piecewise summation of the principal surface stresses obtained from FEA. The algorithm automatically transforms these stresses into an equivalent equibiaxial stress on the glass surface, thereby eliminating the laborious manual calculations associated with this accurate approach. The algorithm accounts for the sub-critical crack growth threshold as well as surface pre-compression arising from the use of heat treated or chemically strengthened glass.

The paper describes the glass strength model and the computer algorithm and its use within the context of a general design methodology for determining the strength of glass. This is followed by a sensitivity analysis and experimental validation.

2. Formulation and application of the glass strength model and the computer algorithm

2.1 Design methodology for determining the tensile strength of glass

The glass design methodology adopted in this paper is based on that proposed by Overend [35] and takes into account the effects of stress history, the stressed surface area and the random orientation of the surface cracks with respect to the principal stresses on the glass surface. This section summarises the main steps of this method (Fig. 4).

Figure 4

Step 1 - The permanent and transient actions on the glass specimen are either known explicitly, or the expected design scenarios can be estimated.

Step 2 – The reference tensile strength of glass net of pre-compression $f_{g,\,t0.\,A0}$, which is associated with an equibiaxial stress state over a reference surface area A_0 for a reference stress duration t_0 , can

be determined either explicitly from known crack geometries, or its characteristic value $f_{gk,\,t0.\,A0}$ can be evaluated by adopting a stochastic strength model based on experimental load test data.

If the physical characteristics and the location of the critical crack on a given surface area of glass A_0 are known, the tensile strength of glass (net of pre-compression) $f_{g,\,t0.\,A0}$ can be evaluated explicitly by extending Eq. (4) to account for the sub-critical crack growth threshold:

$$f_{g,t0,A0} = \left(\sigma_f + f_{rk}\right) = \left\{ \left[\frac{1}{\left(t_0 - t_r\right)} \; \frac{2}{\left(n-2\right) v_0 \; K_{IC}^{-n} \left(Y\sqrt{\pi}\right)^n \; a_i^{(n-2)/2}} \right] \left[\frac{1 - \left(\frac{a_i}{a_f}\right)^{(n-2)/2}}{1 - \left(\frac{a_{TH}}{a_i}\right)^{(n-2)/2}} \right] \right\}^{1/n} \tag{8}$$

Eq. (8) has two asymptotes: the inert strength at very short durations and the threshold strength for very long durations, thereby ensuring that the net crack-opening strength of glass is:

$$\frac{K_{TH}}{Y\sqrt{\pi a_{TH}}} \le \left(\sigma_f + f_{rk}\right) \le \frac{K_{IC}}{Y\sqrt{\pi a_f}} \tag{9}$$

The basis of Eq. (8) is shown in Appendix A and is valid for large values of n, typically n>10. The relationship between the failure stress, the stress duration and the initial flaw size expressed in Eq (8) is plotted in Fig. 5 and Fig. 6 for annealed glass (i.e. $f_{rk} = t_r = 0$) and typical initial crack sizes a_i. The threshold crack size a_{TH} and the critical crack size a_f are obtained by substituting $K_I = K_{TH} = 0.25$ MPa m$^{1/2}$ and $K_I = K_{IC} = 0.75$ MPa m$^{1/2}$, respectively into Eq.(1).

Figure 5

Figure 6

If on the other hand the physical characteristics of the surface cracks are unknown, characteristic tensile strength of glass for a reference test duration t_f (net of pre-compression), $f_{gk,\,tf.\,A0}$ is evaluated statistically, by rearranging Eq. (5):

$$f_{gk,tf,A0} = \left[\frac{-\ln\left(1-P_f\right)}{kA_0}\right]^{1/m} \tag{10}$$

The surface strength parameters m and k are determined from load testing of nominally identical glass specimens with a reference surface area A_0 and a reference test duration t_f and P_f is a suitably low probability of failure. This reference characteristic strength of glass (net of pre-compression) $f_{gk,\,tf.\,A0}$ is specific to the stress duration $(t_f - t_r)$ experienced by the test specimens, but it can be converted to other design lifetimes $(t_0 - t_r)$ by accounting for the sub-critical crack growth that occurs during the period $(t_0 - t_f)$. This can be expressed as:

$$f_{gk,t0,A0} = k_{\mathrm{mod},t}\ f_{gk,tf,A0} \tag{11}$$

where $f_{gk,\,t0,\,A0}$ is the characteristic strength of glass for a reference stress duration $(t_0 - t_r)$ and $k_{mod,\,t}$ is a stress history factor that accounts for the stress corrosion caused by subcritical crack growth that occurs in the period $(t_0 - t_f)$ i.e. $k_{mod,\,t} = 1$ when $t_0 = t_f$.

The stress history factor $k_{mod,\,t}$ can be expressed as the strength relative to the inert strength of glass (i.e. $k_{mod,\,t} = \sigma_{f,\,t0} / \sigma_{f,\,int}$) for a selection of initial flaw sizes a_i, but the inert strength is difficult to determine experimentally, and it has no practical significance in most glass design applications. It is therefore more convenient to set the reference test duration $t_f = 60$s and therefore to describe the stress history factor $k_{mod,\,t}$ with respect to the 60-second strength (Fig. 7).

Figure 7

Step 3 – The principal surface stresses on the glass specimens are determined by means of FEA. The design actions are determined from step 1 and the constitutive material model for glass is isotropic linear elastic. Therefore the principal surface stresses $\sigma_1\,(x, y.\ t)$, will generally vary over time and across the surface of the glass plate.

Step 4 – The principal surface stresses, σ_1 (x ,y. t), are transformed into a an equivalent equibiaxial stress $\sigma_{p,\,t0.\,A0}$ applied for the reference stress duration t_0 and over reference surface area A_0 by modifying Eq. (6). The modification is necessary to account for the onset of sub-critical crack growth which is delayed by the presence of a the sub-critical crack growth threshold, therefore t_r is substituted by t_{TH} and f_{rk} is substituted by (f_{rk} − σ_{TH}):

$$\sigma_{p,t0,\,A0} = \left\{ \frac{1}{A_0} \int_{area} \left[\frac{1}{(t_0 - t_{TH})} \int_{t_{TH}}^{t_d} \left[c_b \sigma_1(x,y,t) + \left(f_{rk}(x.y) - \sigma_{TH} \right) \right]^n dt \right]^{m/n} dA \right\}^{1/m} + \sigma_{TH} \qquad (12)$$

Where A_0 is the reference surface area, dA is the area enclosed by a finite element, σ_1 is the major principal tensile stress in that finite element and σ_{TH} is the stress below which no sub-critical crack growth occurs. The 60s-equivalent stress equibiaxial stress $\sigma_{p,\,t60.\,A0}$ is obtained by setting the reference time t_0 = 60 in Eq. (12).

Step 5 – If the size and location of the critical flaw are unknown the equivalent uniform equibiaxial stress obtained from Eq. (12) is compared to the tensile strength of glass from Eq. (11). If on the other hand, the size and location of the critical flaw are known, the equivalent uniform equibiaxial stress represented by the term in the square brackets of Eq. (6) is compared to the to the tensile strength of glass from Eq. (8).

2.2 Computer algorithm

The computer algorithm is a specially developed subroutine written in visual basic and invoked from the post-processor of the LUSAS FEA software, but it can be easily adapted for other commercial FEA software or to run independently by accessing the FEA results files. The user input to the computer algorithm is interactive wherein the user is prompted to enter the co-ordinates of the glass surfaces and the magnitude of the residual stresses, f_{rk} , resulting from the heat treatment or chemical treatment process (f_{rk} = 0 for annealed glass). The computer algorithm will proceed to calculate the

surface areas, *dA*, and mean principal tensile stresses, σ_1, for each finite element on the specified surface, from which it will then calculate the equivalent uniform stress, $\sigma_{p,\,t0,\,A0}$, for the entire surface by numerical integration of Eq. (12). Finite elements subjected to a net major principle compressive stresses (i.e. $\sigma_1 + (f_{rk} - \sigma_{TH}) < 0$) are automatically eliminated from this calculation.

2.3 Numerical example illustrating the computer algorithm

A 3000mm 2000mm 8mm thick glass plate was analysed using LUSAS v14. The plate was simply supported along its four edges and subjected to a 1kPa uniform lateral load. The plate was modelled with 16 24 mesh consisting of 8-noded, quadrilateral, thin shell elements. A geometrically non-linear analysis with load steps of 100Pa was performed, to capture the nonlinear response resulting from the large deformations of the plate. The major principal stresses, σ_1 obtained from the FEA are shown in Fig. 8.

Figure 8

Since the physical characteristics of the surface cracks were unknown, the tensile strength of glass $f_{gd,\,tf.\,A0}$ was determined statistically. In doing so, the parameters used are those recommended in ASTM E1300 [32]: k =2.86E-53 $m^{-2}Pa^{-7}$; m = 7; n = 16; $t_0 = t_f$ = 3s; $P_f \leq 0.008$.Therefore from Eq. (10), when P_f = 0.008, $f_{gk,\,tf.\,A0} = f_{gk,\,t0.\,A0}$ = 12.46MPa. The equivalent equibiaxial stress $\sigma_{p,\,t0.\,A0}$ on the glass surface is determined by invoking the computer algorithm in the FEA post-processor. This is applied to both surfaces of the plate and yields an equivalent equibiaxial stress, $\sigma_{p,\,t0.\,A0}$ = 11.13MPa and a probability of failure P_f = 0.0072, which is satisfactory. In contrast, the maximum stress approach involves the comparison between the maximum principal tensile stress on the glass surface obtained directly from FEA (which in this case is 15.56MPa) and the limiting characteristic strength $f_{gk,\,t0.\,A0}$, (= 12.46MPa), thereby implying that the design is unsatisfactory. The implicit assumption in the maximum stress approach is that the entire surface area of the glass plate is subjected to the maximum principal stress, which is conservative and would in this instance result in a 416% overestimation of the probability of

failure and a 40% overestimation of the glass thickness when compared to the proposed computer algorithm.

3. Sensitivity Analysis

A parametric analysis was undertaken to assess the sensitivity of the parameters used by the computer algorithm (indicated in Eq. (5) and Eq. (12)) on the equivalent uniform equibiaxial stress and on the resulting probability of failure computed by the algorithm The range of values used in this parametric analysis are based on a number of sources as indicated in Tab.1 and Tab. 2. The reference glass plate used was the 3000mm 2000mm 8mm thick plate described in Section 2.3 with a load duration t_d = 10 minutes.

Table 1, Table 2

Fig. 9 shows the effect in non-dimensional terms of mesh density, load intensity and the statistical parameter *m* on the equivalent uniform stress. The mesh density has a negligible effect on the equivalent uniform stress as long as the FEA solution converges. The graph shows that at higher and lower load intensities the benefit of using the algorithm over the maximum stress approach is even more significant. The plot for the Weibull statistical parameter *m*, which is an inverse measure of the scatter of test data, shows that the equivalent equibiaxial uniform stress $\sigma_{p,\,t0.\,A0}$ drops sharply with a small increase in scatter (i.e. a smaller value of *m*). This is particularly relevant for naturally weathered glass which is generally characterised by a larger scatter of strength data.

Figure 9

As expected the probability of failure P_f is most sensitive to the Weibull statistical parameters as shown in Fig.10. The current lack of test data on naturally weathered glass is therefore problematic. Interestingly, P_f is significantly more sensitive to θ than load intensity. Unsurprisingly, the influence

of the crack velocity parameter *n* on the probability of failure, increases significantly with stress duration.

Figure 10

4. Experimental validation of the computer algorithm

The accuracy of the computer algorithm was assessed by comparing the 2-parameter Weibull distribution predicted by the computer algorithm to that obtained from independently tested glass plates.

4.1 Test data

The test data used for the validation was obtained from tests on four edge supported, 1525mm 2440mm 6mm thick plates of new glass plates carried out by the Ontario Research Foundation (ORF) [47], [48]. This data was selected because the glass was tested at various constant loading rates and the location of the origin of failure was recorded. Furthermore the influence of source variability was also assessed by sourcing the glass from three different suppliers. The total dataset was 145 specimens. Specimens in which failure originated from the glass edges were discarded.

In order to predict the probability of failure, the computer algorithm requires values of the Weibull parameters *m* and *k* as indicated in Eq. (5) and Eq. (12). The parameters were obtained from co-axial double ring (CDR) tests on new glass undertaken by the authors [57]. The CDR specimens were 300mm by 300mm glass plates with a nominal thickness of 3mm. Two sets of rings were used, with loading ring diameters of 51mm and 72.1mm and reaction rings diameters of 127mm and 179.6mm respectively (Fig. 11). This setup creates a quasi-uniform equibiaxial stress state within the loading ring area, making it ideal for assessment of surface strength. Tests were carried out at two different loading rates of 200.14N/min and 20014N/min. A total of 100 specimens of new glass were tested and the location of the failure origin was recorded.

Figure 11

4.2 Data analysis & predictions

The predicted 2-parameter Weibull distribution was determined by substituting the equivalent uniform equibiaxial stress, $\sigma_{p,\,t0.\,A0}$ (with time t_0 = 60s and A_0 = 1m^2) for each CDR specimen into Eq. (5). The equivalent uniform equibiaxial stress, $\sigma_{p,\,t0.\,A0}$ was in turn determined from Eq. (12), with the stress history function $c_b\sigma_1(x, y, t)$ and the time t_d obtained from the CDR test specimens. In this case, the stress history function can be reduced to $\sigma_1(t)$ within the loading ring, but this function is nonlinear due to the large displacements experienced by the CDR test specimens. Fig. 12 shows the CDR test data and the best fit 2-parameter Weibull distribution function, CDR PDF (m = 6.3372 and k = 8.058E-49 m^{-2}Pa$^{-6.3372}$).

The ORF test data were similarly converted to the equivalent uniform equibiaxial stress, $\sigma_{p,\,t0.\,A0}$ (with time t_0 = 60s and A_0 = 1m^2). This was done by deploying the computer algorithm on the FEA of the ORF glass plates as described in the numerical example in Section 2.3. The equivalent ORF test data and the resulting best-fit 2-parameter Weibull distribution, ORF PDF (m = 6.4134 and k = 1.01E-49m^{-2}Pa$^{-6.4134}$) are superimposed on Fig 12. The maximum principal tensile stress at failure of the ORF specimens is also shown in Fig. 12. The effect of the sub-critical crack growth threshold on probability of failure for such short load durations, often used to characterise wind loading scenarios, was found to be negligible. This was determined by assessing the effects on crack growth of a time history of wind pressures measured in full scale [57]. The effects of the crack growth threshold are however expected to become significant, when considering long duration loads such as the self-weight of glass in horizontal glazing.

Figure 12

4.3 Comparisons and comments

The PDF obtained from the CDR tests data provides a close yet safe prediction of the ORF large panel test data. The difference between the predicted and reported PDFs may be attributed to the differences in the sources and surface quality of the two glass populations. The differences are however small and demonstrate the accuracy of the algorithm in converting between different states of stress, stress histories and surface areas. In contrast the maximum stress approach would in this instance provide an artificially high and unsafe estimate of glass strength.

5. Conclusions

The computationally simple way to determine the tensile strength of a glass element is to adopt a maximum stress approach whereby the maximum stress obtained from structural analysis is assumed to be acting over the whole surface of the glass plate. This approach was shown to be inaccurate and unduly conservative in estimating the failure stress of glass. Conversely, the maximum stress approach could yield unsafe results when used for the statistical interpretation of laboratory tests.

There are two alternative approaches that can be used to predict the extrinsic strength of glass. In the first approach the strength of glass may be determined explicitly form the characteristics of the critical flaw. The second approach is stochastic and is used when the critical flaw characteristics are unknown.

The explicit approach has been extended in this paper to include both the inert strength limit and the sub-critical crack growth threshold. Sub-critical crack growth affects the lifetime of glass plates, but the sub-critical crack growth threshold was found to have a negligible effect for typical wind loading scenarios. The presence of a sub-critical crack growth threshold will be significant when considering long duration loads. Further experimental validation of sub-critical crack growth, particularly for long stress durations, is therefore required. These investigation should include investigations on low frequency cyclic loads to determine the extent of, and the conditions that give rise to, crack healing in soda lime glass.

The stochastic approach is unattractive for manual computation as it involves the conversion of the surface stresses to an equivalent uniform equibiaxial stress. The computer algorithm described in this paper overcomes this problem by using the results from commercially available FEA software and automating the calculation. This paper shows that the computer algorithm provides accurate and safe predictions of glass strength. Furthermore it has been shown that test data from small scale specimens such as coaxial double ring tests can be used to predict the strength of much larger glass plates with different load histories, and boundary conditions. The use of the computer algorithm would in practice result in a safer and more efficient use of glass, and its speed and accuracy may be exploited for the structural optimisation of more complex glass applications.

It was also shown that for uniformly loaded glass plates the computer algorithm is not sensitive to the density of the finite element mesh, but as expected, the algorithm is sensitive to the statistical Weibull parameters (m and k) that characterise glass strength. The significant discrepancies in the values of these parameters reported in literature and the paucity of weathered glass test data indicate that the computer algorithm should be used with caution. Further research on new and naturally weathered glass is required to improve the confidence in the statistical Weibull parameters and to improve the interpretation of laboratory test results. The use of the computer algorithm for concentrated loads and point supports should also be investigated further.

Appendix A Strength *vs.* time relationship of a single crack

This appendix shows the derivation of Eq. 8 that expresses the tensile strength of glass as a function of the stress history on a single flaw.

Irwin [3] described the stress intensity at the crack tip in terms of the stress intensity factor, K, which for mode I loading is:

$$K_I = Y\sigma\sqrt{\pi a} \tag{A1}$$

Where σ is the tensile stress normal to the crack, a is the crack depth or half the crack length and Y is a geometry factor that describes the crack geometry and the proximity of the specimen boundaries. Fast fracture occurs when the critical stress intensity factor is exceeded (i.e. $K_I > K_{IC}$):

$$K_{IC} = Y\sigma\sqrt{\pi a_f} \tag{A2}$$

Where a_f denotes the critical flaw depth (or half its length) required to cause fast fracture. Making σ the subject of the formula in Eq. A2 yields the inert strength ($\sigma = \sigma_{int}$) i.e. the resistance to fast fracture that is independent of stress history and environmental conditions. However, sub-critical crack growth occurs in the region $K_I \leq K_{IC}$. Furthermore, at stress intensities below the sub-critical crack growth threshold K_{TH} no crack growth occurs such that

$$K_{TH} = Y\sigma\sqrt{\pi a_{TH}} \tag{A3}$$

where a_{TH} is the flaw depth (or half the flaw length) below which no crack growth occurs. Similarly Eq. (A3) quantifies the threshold stress ($\sigma = \sigma_{TH}$) below which no crack growth occurs. This is expressed as a discontinuity in the *v*-*K* relationship (Fig. A1).

Figure A1

Munz and Fett [7] showed that the sub-critical crack velocity i.e. the crack velocity at stress intensities $K_I \leq K_{IC}$ can be expressed as:

$$v = v_0\left(K_I / K_{IC}\right)^n \tag{A4}$$

where n is the crack velocity parameter (also known as the static fatigue constant). The ordinary differential equation for crack growth is therefore obtained by substituting Eq. (A1) into Eq. (A4):

$$\frac{da}{dt} = v = v_0 \left(\frac{Y\sigma(t)\sqrt{\pi a}}{K_{IC}} \right)^n \tag{A5}$$

For accurate lifetime predictions, the crack velocity v, should be limited to region I; a constant velocity should be used for region II and a different velocity should be adopted for region III. Such an approach is proposed for the proof testing of ceramics [58]. However since the crack is travelling relatively fast in regions II and III, the contribution to the lifetime as it traverses these regions is small and may be conservatively estimated by assuming Eq. 1 is valid for $K_{TH} \leq K_I \leq K_{IC}$ and that n is constant over the three regions (Fig A1). This simplification was suggested by Wachtman [6], and Munz & Fett [7] for the lifetime prediction of ceramics and was implemented by Haldimann [15] for the lifetime prediction of glass. Rearranging Eq. (A5) and introducing the surface pre-compression f_{rk} induced by heat or chemical treatment and t_r, the time at which the applied stress $\sigma + f_{rk} = 0$:

$$\int_{a_i}^{a} a^{-n/2} da = v_0 \left(Y\sqrt{\pi} \right)^n K_{IC} \int_{t_r}^{t} (\sigma + f_{rk})^n (t) dt \tag{A6}$$

Where a_i is the initial flaw size (at time t = 0) and a is the flaw size at time t. By integrating the left side of Eq. (A6) and rearranging we can obtain a general expression for the time dependant size of a crack exposed to a net crack opening stress ($\sigma + f_{rk}$):

$$\int_{t_r}^{t} (\sigma + f_{rk})^n (t) dt = \frac{2}{(n-2)\, v_0\, K_{IC}^{-n} \left(Y\sqrt{\pi} \right)^n a_i^{(n-2)/2}} \left[1 - \left(\frac{a_i}{a} \right)^{(n-2)/2} \right] \tag{A7}$$

For $a_i \vee a$, $(a/a_i)^{(n-2)/2} \rightarrow 0$, therefore Eq (A7) simplifies to:

$$\int_{t_r}^{t} (\sigma + f_{rk})^n (t) dt = \frac{2}{(n-2)\, v_0\, K_{IC}^{-n} \left(Y\sqrt{\pi} \right)^n a_i^{(n-2)/2}} \tag{A8}$$

No crack growth occurs below the sub-critical crack growth threshold i.e. when $a_i \leq a_{TH}$. This is particularly relevant in the region $a_i \approx a_{TH}$ (i.e. $a_i \vee a_f$). Eq. (A8) may therefore be modified to account for the sub-critical crack growth threshold:

$$\int_{t_r}^{t} (\sigma + f_{rk})^n (t) dt = \frac{2}{(n-2) v_0 K_{IC}^{-n} \left(Y\sqrt{\pi}\right)^n \left(a_i^{(n-2)/2} - a_{TH}^{(n-2)/2}\right)} \tag{A9}$$

This is valid when n is large and when $a_{TH} << a_f$ which is typical of soda-lime-silica glass. Eq. (A9) effectively eliminates subcritical crack growth when $K_I \leq K_{TH}$ whilst maintaining the *v*-*K* relationship in the range $K_{TH} < K_I < K_{IC}$ (Fig. A1). Eq.(A9) may be re-written as:

$$\int_{t_r}^{t} (\sigma + f_{rk})^n (t) dt = \frac{2}{(n-2) v_0 K_{IC}^{-n} \left(Y\sqrt{\pi}\right)^n a_i^{(n-2)/2}} \cdot \frac{1}{\left[1 - \left(a_{TH}/a_i\right)^{(n-2)/2}\right]} \tag{A10}$$

The combination of Eq. (A7) and Eq. (A10) provides a unified expression for lifetime prediction:

$$\int_{t_r}^{t} (\sigma + f_{rk})^n (t) dt = \left[\frac{2}{(n-2) v_0 K_{IC}^{-n} \left(Y\sqrt{\pi}\right)^n a_i^{(n-2)/2}} \right] \left[\frac{1 - \left(\frac{a_i}{a}\right)^{(n-2)/2}}{1 - \left(\frac{a_{TH}}{a_i}\right)^{(n-2)/2}} \right] \tag{A11}$$

For a net crack opening stress applied constantly until failure $\sigma = \sigma_f$; $t = t_f$; $a = a_f$:

$$t_f - t_r = \frac{1}{(\sigma_f + f_{rk})^n} \frac{2}{(n-2) v_0 K_{IC}^{-n} \left(Y\sqrt{\pi}\right)^n a_i^{(n-2)/2}} \left[\frac{1 - \left(\frac{a_i}{a_f}\right)^{(n-2)/2}}{1 - \left(\frac{a_{TH}}{a_i}\right)^{(n-2)/2}} \right] \tag{A12}$$

This is asymptotic to inert strength, i.e.$(t_f - t_r) \rightarrow 0$ as $a_i \rightarrow a_f$, and asymptotic to the threshold strength, i.e. .$(t_f - t_r) \rightarrow$: as $a_i \rightarrow a_{TH}$ (Fig. A2). Eq. (8) is expressed in term of a reference stress duration, by substituting t_0 for t_f in Eq. (A12).

Figure A2

A useful result from Eq. (A11) is the crack size a for a known stress history:

$$a = \left\{ a_i^{(2-n)/2} - \left[1 - \left(\frac{a_{TH}}{a_i} \right)^{(n-2)/2} \right] \cdot \frac{(n-2) v_0 \, K_{IC}^{-n} \left(Y\sqrt{\pi} \right)^n}{2} \cdot \int_{t_r}^{t} \left(\sigma + f_{rk} \right)^n (t) dt \right\}^{2/(2-n)} \quad \text{(A13)}$$

Acknowledgements

We are grateful to the Southwest Research Institute, San Antonio, Texas, US, for providing a copy of the NASGRO v6.2 for evaluation. The NASGRO software suite was developed by the NASA Johnson Space Center and Southwest Research Institute. Thanks are also due to the Connecticut Reserve Technologies Inc., Ohio, US, for providing a copy of the CARES software for evaluation. The software was originally developed by the Life Prediction Branch of the NASA Glenn Research Center.

References

[1] Shelby JE. Introduction to Glass Science and Technology, Royal Society of Chemistry, Cambridge; 1997.

[2] Overend M, De Gaetano S, Haldimann M. Diagnostic Interpretation of Glass Failure. Structural Engineering International 2007;17(2):151–158.

[3] Irwin G. Analysis of Stresses and Strains near the End of a Crack Traversing a Plate. Journal of Applied Mechanics 1957;24:361–364.

[4] Haldimann M, Luible A, Overend M. Structural use of glass. Structural Engineering document no. 10, International Association of Bridge and Structural Engineers; 2008.

[5] Uhlmann DR, Kreidl NJ eds. Glass Science and Technology: Volume 5, Elasticity and Strength in Glasses. Academic Press; 1980.

[6] Wachtman JB. Mechanical Properties of Ceramics. Wiley Interscience; 1996.

[7] Munz D, Fett T. Ceramics: Mechanical properties, failure behaviour, materials selection. Springer; 1999.

[8] Kurkijan CR, Gupta PK, Brow RK, Lower N. The intrinsic strength and fatigue of oxide glasses. J Non Cryst Solids 2003;316(1):114-124.

[9] Grenet L. Mechanical Strength of Glass. Enc. Industr. Nat. Paris 1899;5(4):838–848.

[10] Mould RE, Southwick RD. Strength and static fatigue of abraded glass under controlled ambient conditions: I, General concepts and apparatus. J. Am Ceram, Soc. 1959;42:542-547.

[11] Mould RE, Southwick RD. Strength and static fatigue of abraded glass under controlled ambient conditions: II, Effect of various abrasions and the universal fatigue curve. J. Am Ceram, Soc. 1959;42:582-592.

[12] Wiederhron SM. Influence of water vapor on crack propagation in soda-lime glass. J. Am Ceram, Soc. 1967;50:407-414.

[13] Michalske TA, Freiman SWA. Molecular Mechanism for Stress Corrosion in Vitreous Silica. J. Am Ceram. Soc. 1983;66:284–288.

[14] Evans AG, Wiederhorn SM. Proof testing of ceramic materials – an analytical basis for failure prediction. Int. J. of Fracture 1974;10(3):379–392.

[15] Haldimann M. Fracture Strength of Structural Glass Elements – Analytical and numerical modelling, testing and design. Thèse EPFL No 3671, Ecole polytechnique fédérale de Lausanne (EPFL); 2006.

[16] Charles RJ, Hillig WB. The kinetics of glass failure by stress corrosion. In: Symposium on Mechanical Strength of Glass and Ways of Improving it, Charleroi, Belgium 1962; 25-29.

[17] Wiederhorn SM, Johnson H. Effect of electrolyte pH on crack propagation in glass. J. Am. Ceram. Soc. 1973;56:192–197.

[18] Wiederhorn SM, Bolz LH. Stress corrosion and static fatigue of glass. J. Am. Ceram. Soc. 1970;53:543–548.

[19] Wilkins BJS, Dutton R. Static Fatigue Limit with Particular Reference to Glass. J. Am. Ceram. Soc, 1976;59:108–112.

[20] Gehrke E, Ullner C, Hähnert M. Fatigue limit and crack arrest in alkali-containing silicate glasses. Journal of Materials Science 1991;26:5445–5455.

[21] Guin JP, Wiederhorn S. Crack growth threshold in soda lime silicate glass: role of hold-time. Journal of Non-Crystalline Solids 2003;316(1):12–20.

[22] Evans AG. A method for evaluating the time-dependent failure characteristics of brittle materials and its application to polycrystalline alumina. J Mat. Sci. 1972;7(10):1137-1146.

[23] Brown WG. A practicable formulation for the strength of glass and its special application to large plates. Publication No. NRC 14372, National Research Council of Canada, Ottawa; 1974.

[24] Beason WL, Morgan JR. Glass Failure Prediction Model. ASCE J. Struct. Eng. 1984;110(2):197-212.

[25] Sedlacek G, Blank K, Gusgen J. Glass in structural engineering. The Structural Engineer 1995; 73(2):17-22.

[26] Fischer-Cripps A.C, Collins R.E. Architectural glazing: Design standards and failure models. Building and Environment 1995;30(1):29-40.

[27] Porter MI, Houlsby GT. Development of crack size limit state design methods for edge-abraded glass members. The Structural Engineer 2001; 79(8), 29-35.

[28] Overend M, Parke, GAR. Buhagiar D. A general crack growth model for predicting failure in glass, ASCE J. Struct. Eng. 2007; 133(8):1146-1155.

[29] Green DJ, Dwievedi PJ, Sglavo V M. Characterisation of subcritical crack growth in ceramics using indentation cracks. British Ceramic Transactions 1999;98(6):291-295.

[30] NASGRO v6.2 Fracture Mechanics and Fatigue Crack Growth Analysis Software. NASA Johnson Space Center and Southwest Research Institute; 2011.

[31] CAN/CGSB 12-20-M89. Structural design of glass for buildings. National Standard of Canada. Canadian General Standards Board; 1989.

[32] ASTM E 1300–09a. Determining Load Resistance of Glass in Buildings. Philadelphia, USA; 2009.

[33] CEN prEN13474. Glass in Building – Design of Glass Panes – Part 1: General Basis of Design. European Committee for Standardisation, Brussels; 2007.

[34] Behr RA, Karson MJ, Minor JE. Reliability Analysis of Window Glass Failure Pressure Data. Structural Safety 1991;11:43-58.

[35] Overend. M. Recent developments in design methods for glass structures, The Structural Engineer, Volume 88, Issue14, 18-26, 2010.

[36] Laufs W, Sedlacek G. Stress distribution in thermally tempered glass panes near the edges, corners and holes; Part 2. Distribution of thermal stresses. Glass Science and Technology 1999; 72(2), 42-48.

[37] Norville HS, Bove PM, Sheridan DL. The strength of new thermally tempered window glass lites, Glass Research and Testing Lab. Texas Tech University, USA. 1991.

[38] SJ MEPLA version 3.5.4. Software for structural glass design. http://www.mepla.eu. 2011.

[39] Overend M. The appraisal of structural glass assemblies. PhD thesis, University of Surrey UK, 2002.

[40] Connecticut Reserve Technologies. Ceramic Analysis and Reliability Evaluation of Structures (CARES) v. 9.1.0.181. http://www.ceramicreliability.com/software/cares.html. 2011

[41] Nemeth N, Powers LM, Janosik LA, Gyekenyesi JP. CARES/LIFE Ceramics Analysis and Reliability Evaluation of Structures Life Prediction Program. NASA/TM—2003-106316, 2003.

[42] Batdorf SB, Heinisch HL. Weakest link theory reformulated for arbitrary fracture criterion. J. Am. Ceram. Soc.1978;61(7-8):355-358.

[43] Gross B, Powers, LM, Jadaan OM, Janosik LA. Fatigue parameter estimation methodology for power and Paris crack growth laws in monolithic ceramic materials. NASA/TM-4699; 1996.

[44] DIN 1249-10:1990. Flachglas im Bauwesen – Teil 10: Chemische und physikalische Eigenschaften; 1990.

[45] Fink A. Ein Beitrag zum Einsatz von Floatglas als dauerhaft tragender Konstruktionswerkstoffim Bauwesen. Ph.D. thesis, Technische Hochschule Darmstadt, 2000.

[46] Ritter JE, Service TH, Guillemet C. Strength and fatigue parameters for soda-lime glass. Glass Technology 1985;26(6):273–278.

[47] Johar S. Dynamic fatigue of flat glass – Phase II. Technical Report, Ontario Research Foundation. Department of Metals, Glass and Ceramics, Missisagua, Canada; 1981.

[48] Johar S. Dynamic fatigue of flat glass – Phase III. Technical Report, Ontario Research Foundation. Department of Metals, Glass and Ceramics, Missisagua, Canada; 1982.

[49] Kerkhof F, Richter H, Stahn D. Festigkeitvon Glas – Zur Abhängigkeit von Belastungsdauer und –verlauf. Glastechnische Berichte 1981;54(8):265–277.

[50] Sglavo V, Bertoldi M. Vickers indentation: a powerful tool for the analysis of fatigue behavior on glass. Ceramic Transactions 2004;156:13-22.

[51] Sglavo V, Gadotti M, Micheletti. T. Cyclic loading behaviour of soda lime silicate glass using indentation cracks. Fatigue Fract. Eng. Mater. Struct. 1997; 20(8):1225–1234.

[52] Sglavo V. and Green D. J. Indentation fatigue testing of soda-lime silicate glass. J. Mat. Sci. 1999;34(3):579–585.

[53] Dwivedi P, Green DJ. Determination of subcritical crack growth parameters by in situ observations of indentation cracks. J. Am. Ceram. Soc. 1995;78(8):2122-2128.

[54] Schneider J. Festigkeit und Bemessung punktgelagerter Gläser und stossbeanspruchter Gläser. Ph.D. thesis, TU Darmstadt, Institut für Statik; 2001.

[55] Choi SR, Holland F. Dynamic fatigue behavior of soda-lime glass disk specimens under biaxial loading. NASA Lewis Research Center, Cleveland, Ohio; 1994.

[56] Mencík, J. Strength and fracture of glass and ceramics. Elsevier, New York; 1992.

[57] Zammit K. and Overend M. Increasing the design strength of glass – fractography and stress testing. Proceedings of the International Association for Shell and Spatial Structures Symposium, Valencia, Spain. September 2009.

[58] Fuller E. R., Wiederhorn S. M., Ritter J. E., Oates P. B. Proof testing of ceramics. Journal of Materials Science, 15 (9), p 2282-2295, 1980.

Table 1

Test Source	m	$\theta_{60s,\ 1sq.m}$ (MPa)	f_{gk} @ P_f=0.05 (MPa)
Brown [23]	7.30	51.44	34.2
Beason & Morgan [24]	9.00	45.01	32.4
DIN 1249-10 [42]	5.65	46.72	27.6
Fink [43]	7.20	45.62	30.2
Ritter *et al.* [44]	7.14	46.75	33.9
Johar [45] @ 0.15 kPa/s	7.11	47.43	31.2
Johar [45] @ 1.5 kPa/s	6.54	47.23	31.0
Johar [45] @ 15 kPa/s	7.38	42.70	28.5
Johar [46] @ 0.0025 kPa/s	6.63	43.35	27.7
Johar [46] @ 0.025 kPa/s	6.41	43.62	27.5
Johar [46] @ 0.25 kPa/s	9.67	46.23	33.3
Johar [46] @ 2.5 kPa/s	5.01	47.15	26.1
Haldimann [15] – Inert testing	8.21	49.74	34.6
This Study	6.34	38.83	24.3

Table 2

Source	Conditions	*n*
Kerkhof *et al.* [47]	Water	16.0
Kerkhof et al. [47]	Air 50% RH	18.1
Sglavo & Bertoldi [48]	Water - dynamic fatigue tests	26 ±7
Sglavo *et al.* [49]	Water - cyclic fatigue tests	18 ±1
Sglavo & Green [50]	Water - dynamic fatigue tests on indented glass	20.1 ± 0.7
Sglavo & Green [50]	Water - dynamic fatigue tests on annealed glass	19.9 ± 0.7
Dwivedi & Green [51]	Air 27°C 65% RH - direct optical measurement	19.7 to 21.2
Dwivedi & Green [51]	Air 27°C 65% RH - 4PB dynamic fatigue, natural flaws	21.8
Dwivedi & Green [51]	Air 27°C 65% RH - 4PB dynamic fatigue, indentation flaws	21.1
Schneider [52]	Dynamic fatigue tests	17 to 21
Fink [43]	Static Fatigue in open air and in a climate chamber	16.0
Choi & Holland [53]	Dynamic fatigue tests	16.4
Mencik [54]	Review of published data	12 to 17
Sedlacek *et al.* [25]	Liquid water at 25°C	16.0
Sedlacek *et al.* [25]	Air 25°C 50% RH	18.1
Sedlacek *et al.* [25]	Air 25°C 10% RH	27.0
Sedlacek *et al.* [25]	Inert, dry environment at 25°C	70.0
Sedlacek *et al.* [25]	Melting Snow at 2°C	16.0

Figure & Table Captions

Fig. 1. Clamp-supported glass at 2200 Pennsylvania Avenue, New York (courtesy Thornton Tomasetti).

Fig. 2. Bolted glass fins at Marriott Hotel, Kensington, London (courtesy Pilkington, NSG Group).

Fig. 3. Micrograpgh of 20-year old weathered float glass surface taken with polarised light microscope.

Fig. 4. Methodology for structural design (tensile strength) of glass.

Fig. 5. Failure stress *vs.* stress duration for a range of initial flaw sizes $a_i \geq .50\mu m$.

Fig. 6. Failure stress *vs.* stress duration for a range of initial flaw sizes $a_i \leq 50\mu m$.

Fig. 7. Relative strength *vs.* stress duration for a range of initial flaw sizes. Relative strength is expressed w.r.t. 60s i.e. = $k_{mod,\,t60} = (\sigma_f / \sigma_{t60})$.

Fig. 8. Principal stress contours on the loaded surface of the 3000mm x 2000mm x 8mm glass plate. Uniformly distributed load and boundary conditions not shown for clarity.

Fig. 9. Equivalent equibiaxial stress / Maximum principal stress ($\sigma_{p,\,tf.\,A0} / \sigma_1$) *vs.* Reference parameter.

Fig. 10. Probability of failure *vs.* Reference parameter.

Fig. 11. Co-axial double ring (CDR) test set-up.

Fig. 12. Probability of failure *vs.* 60s equivalent failure stress.

Fig. A1. Idealised v-K relationship.

Fig A2. Failure stress of a surface crack as a function of stress duration.

Table 1. Strength parameters for new, as received glass ($\theta = 1/(Ak)^{1/m}$ in MPa).

Tab. 2. Crack growth parameter, *n*.

Figure 1
Click here to download high resolution image

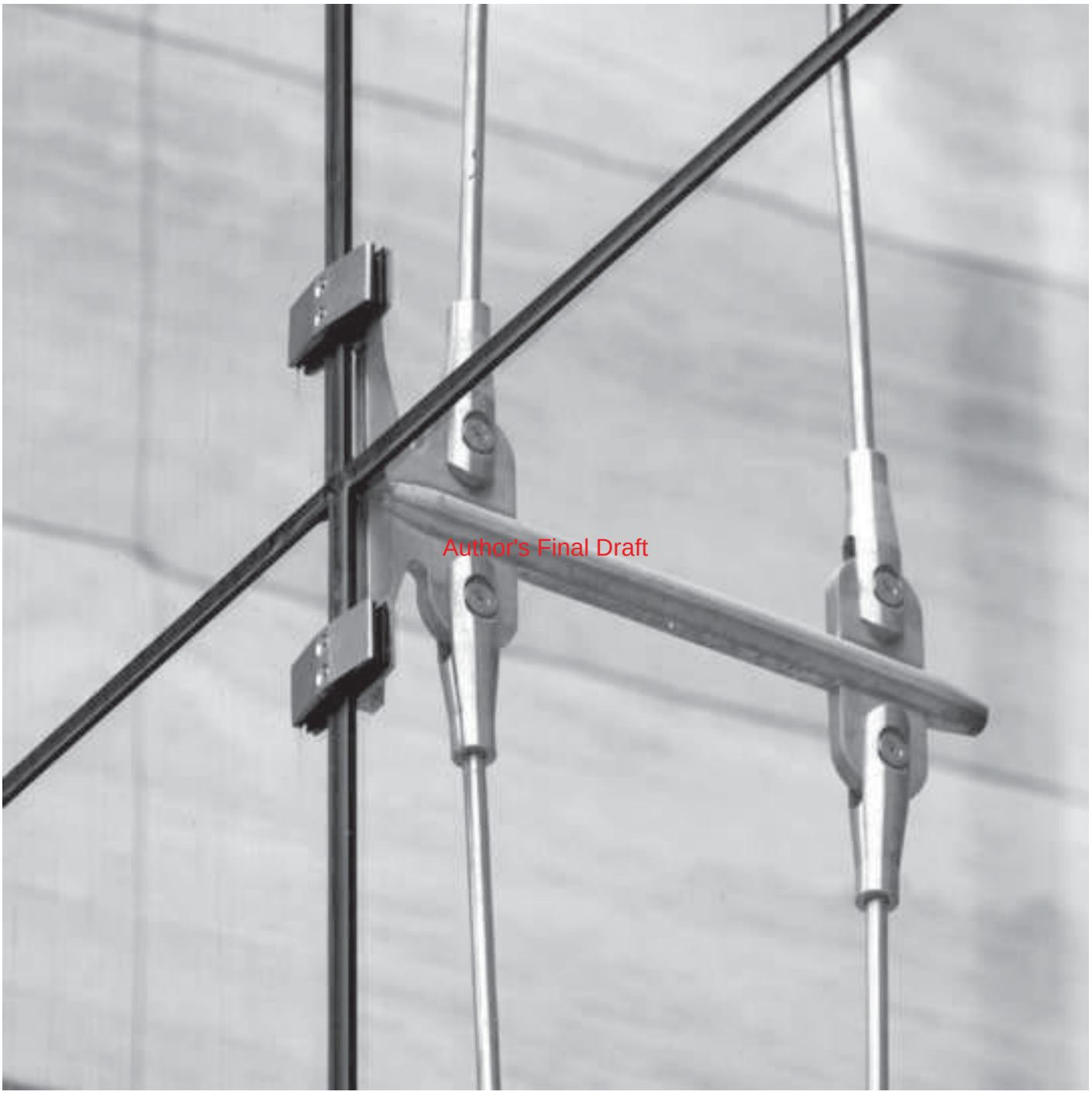

Figure 2
Click here to download high resolution image

Figure 3

Click here to download high resolution image

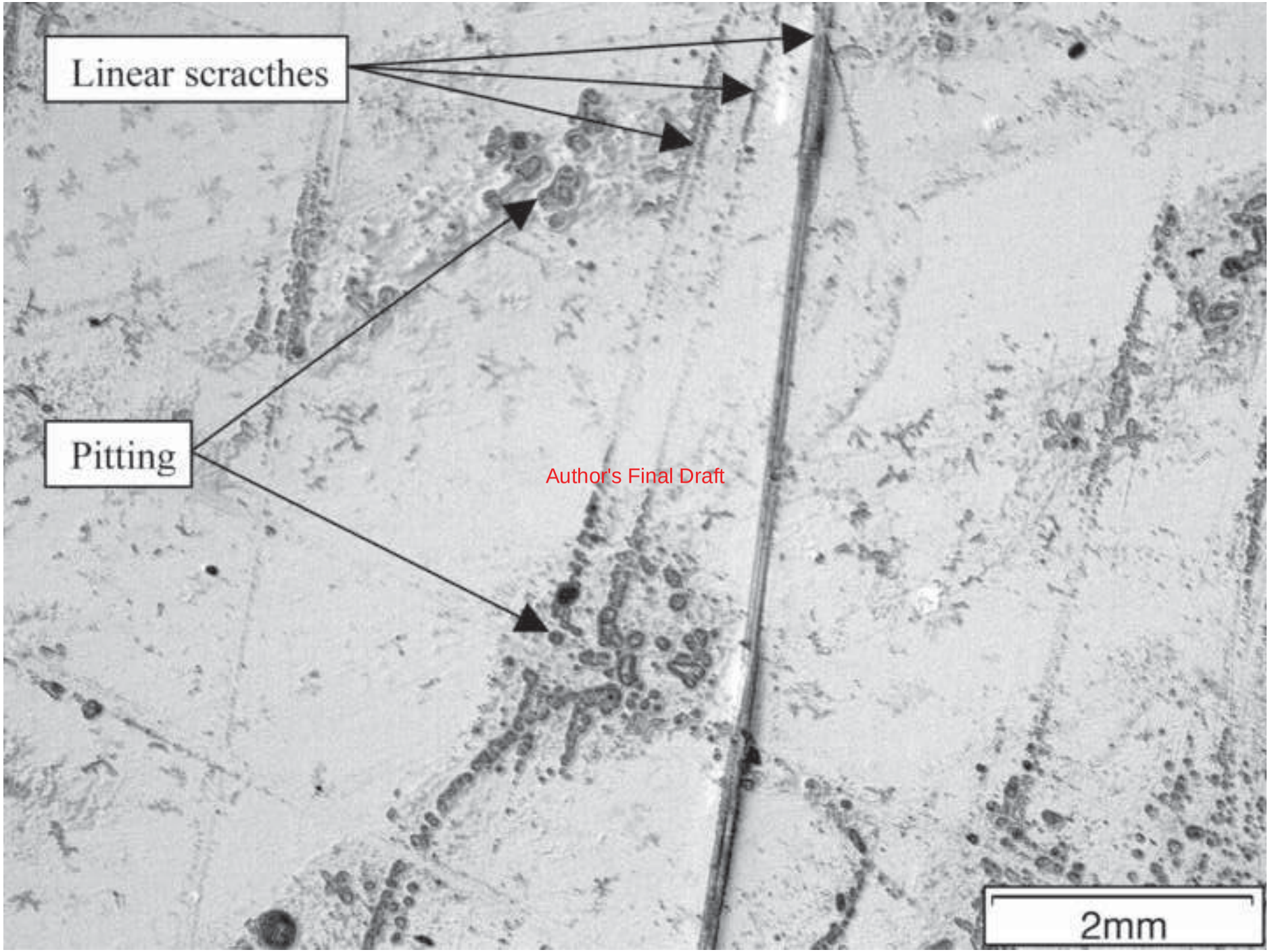

Figure 4
Click here to download high resolution image

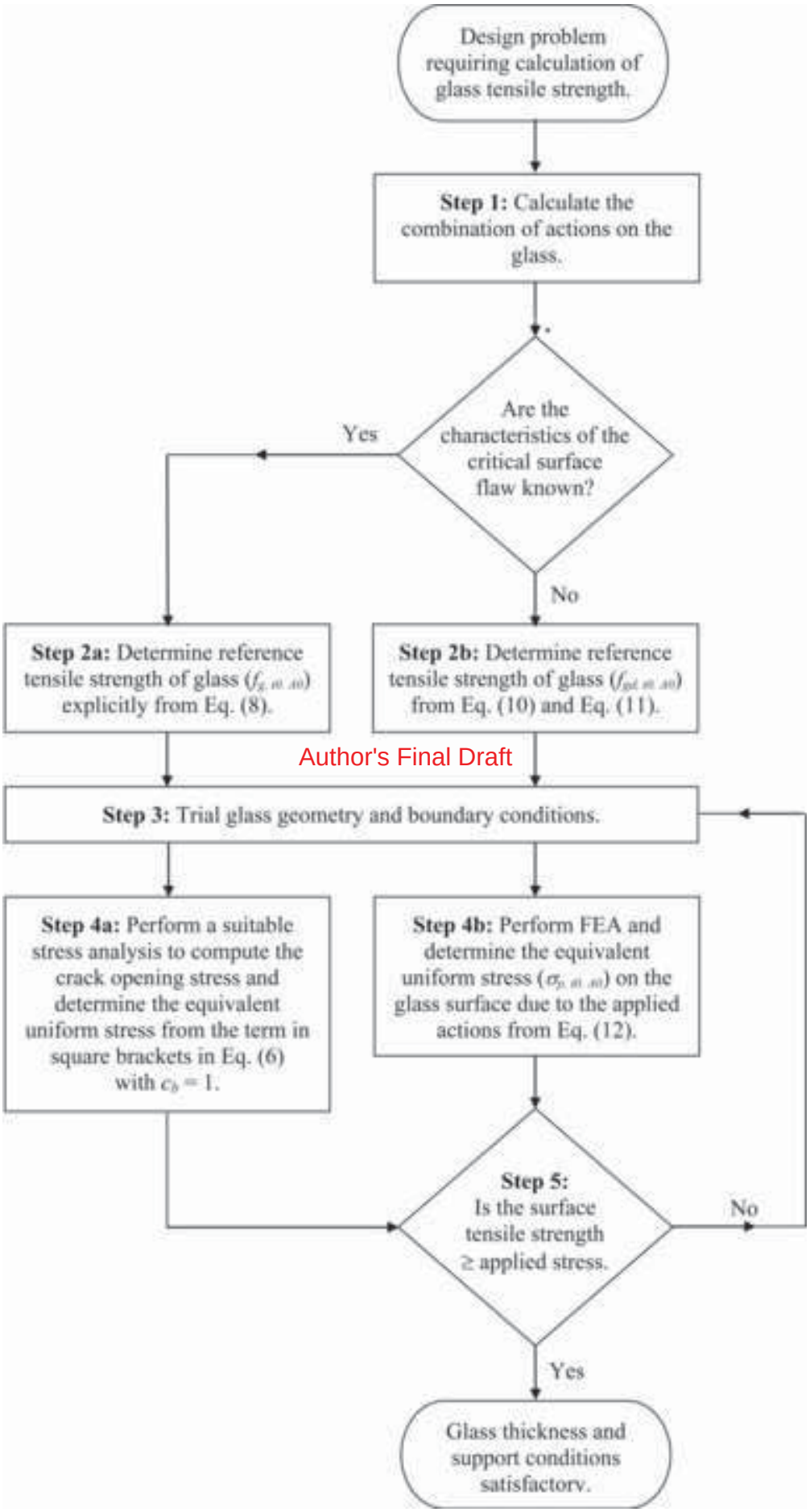

Figure 5

Click here to download high resolution image

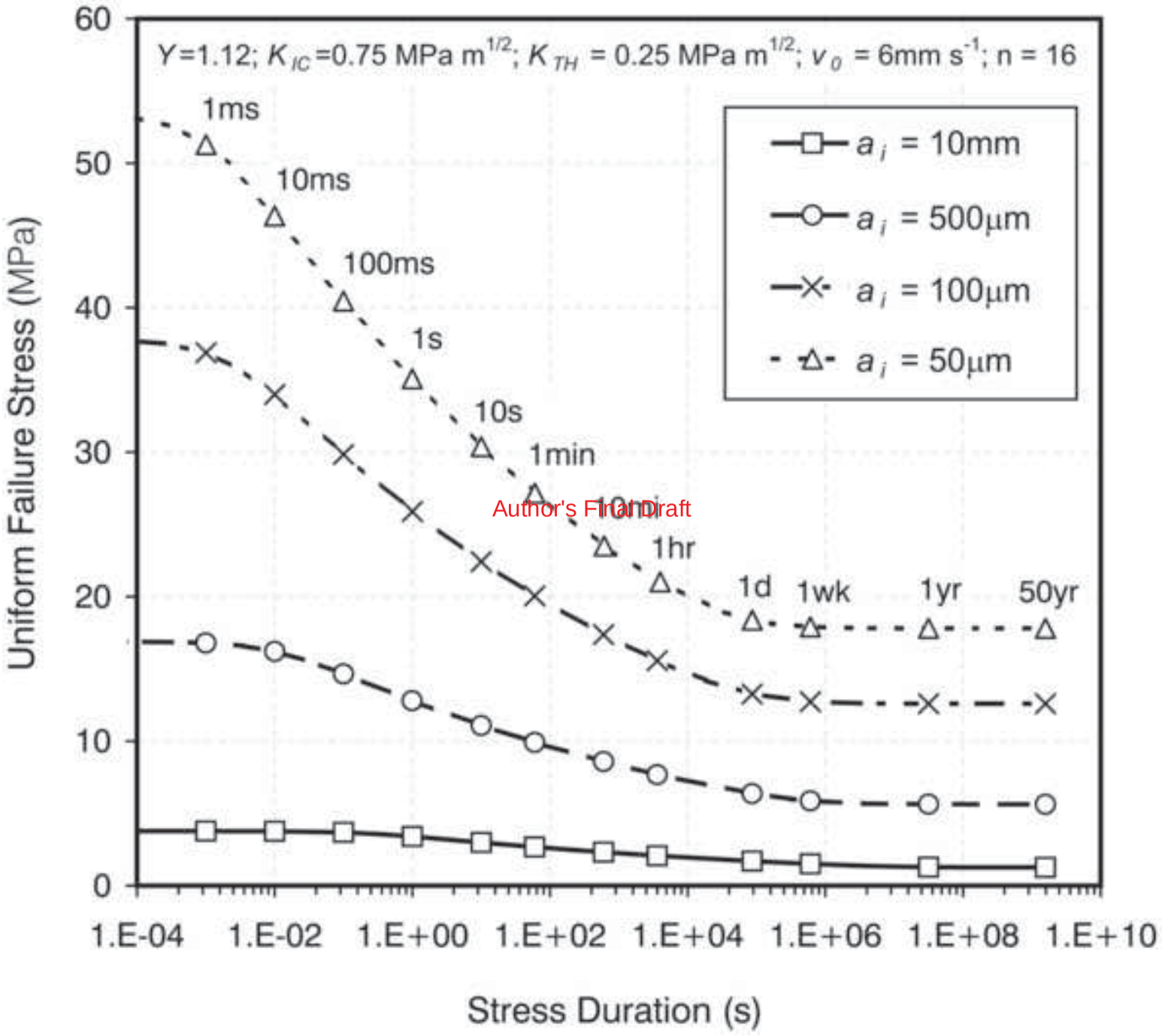

Figure 6

Click here to download high resolution image

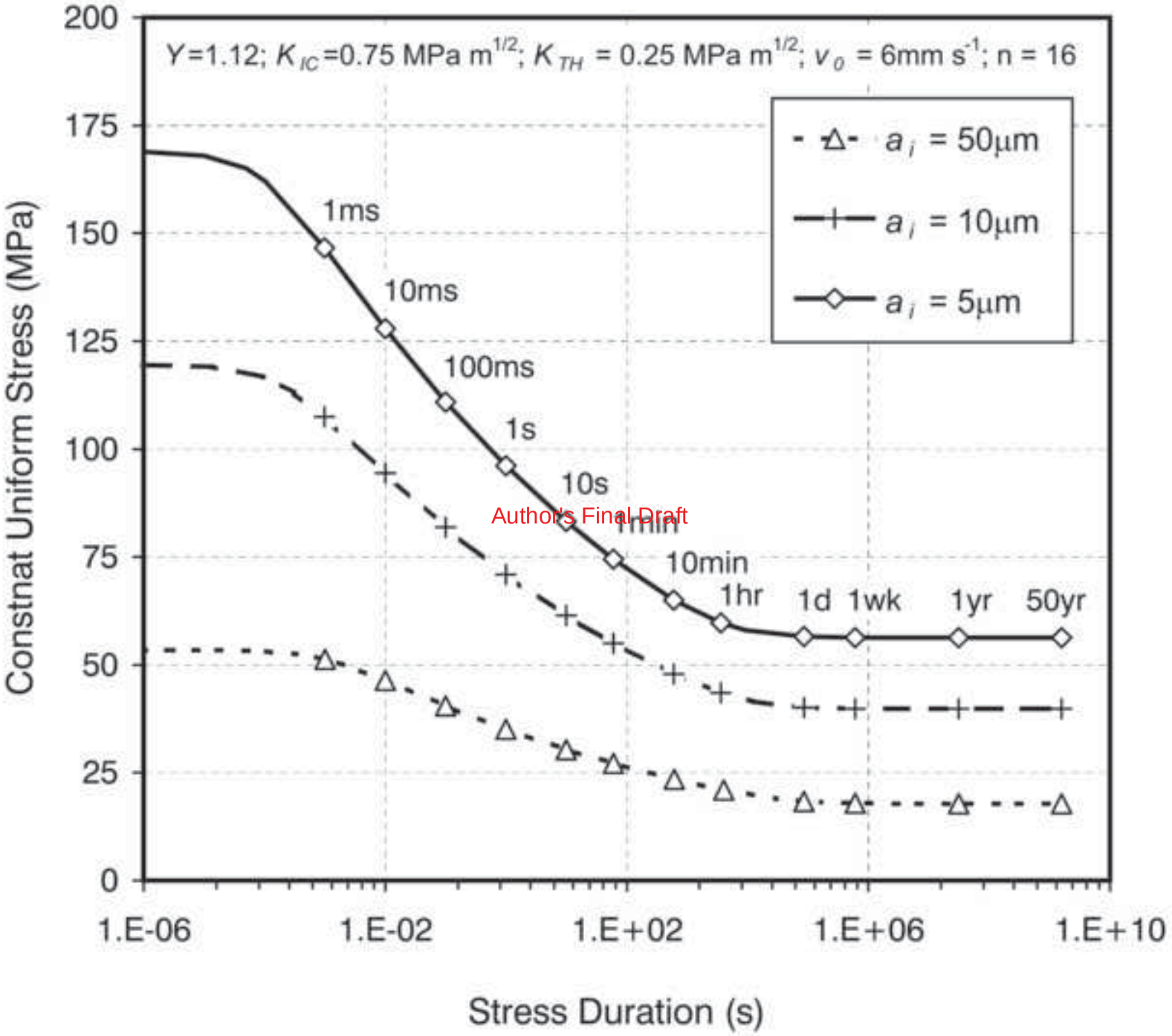

Figure 7

Click here to download high resolution image

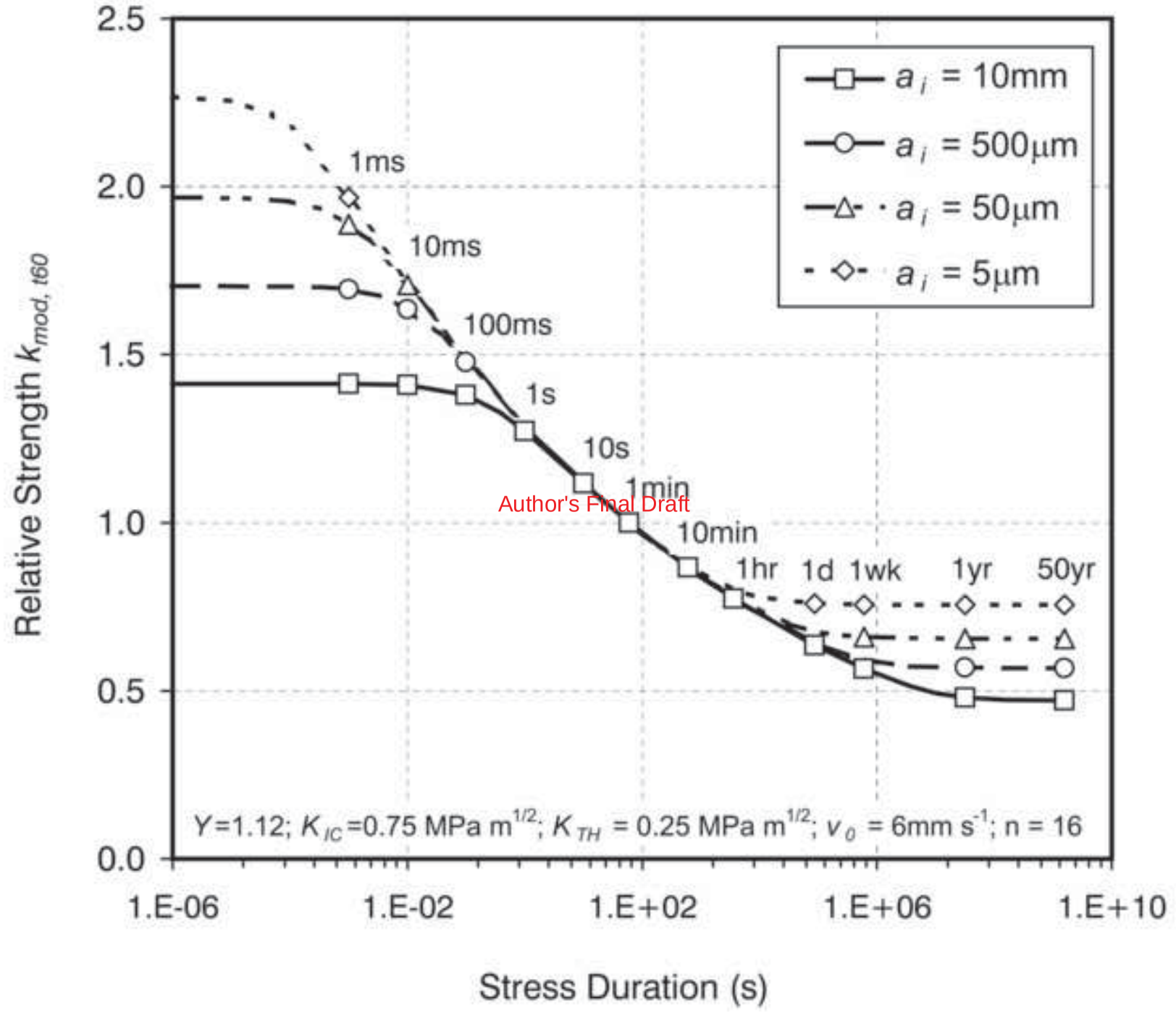

Figure 8
Click here to download high resolution image

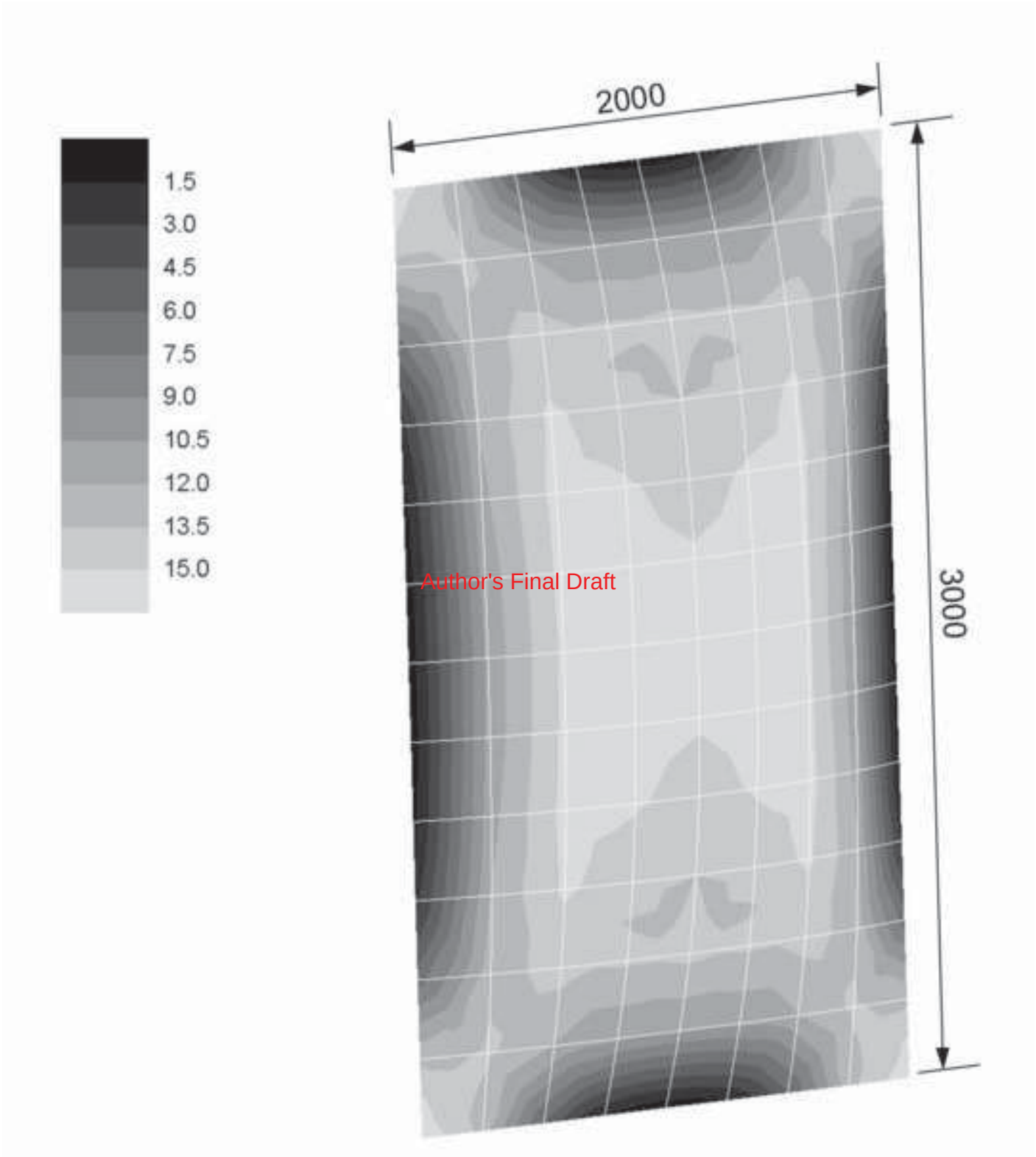

Figure 9

Click here to download high resolution image

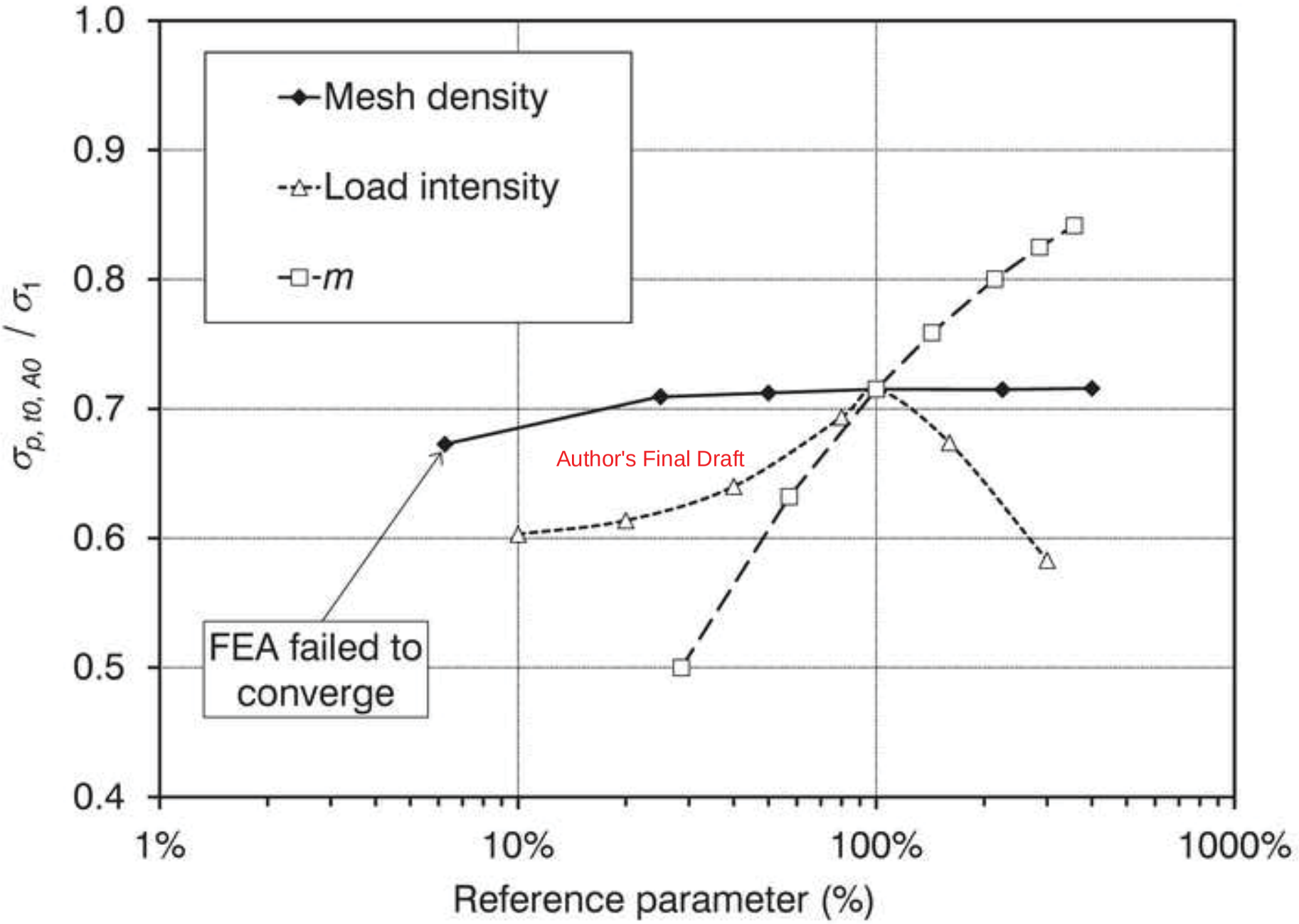

Figure 10
Click here to download high resolution image

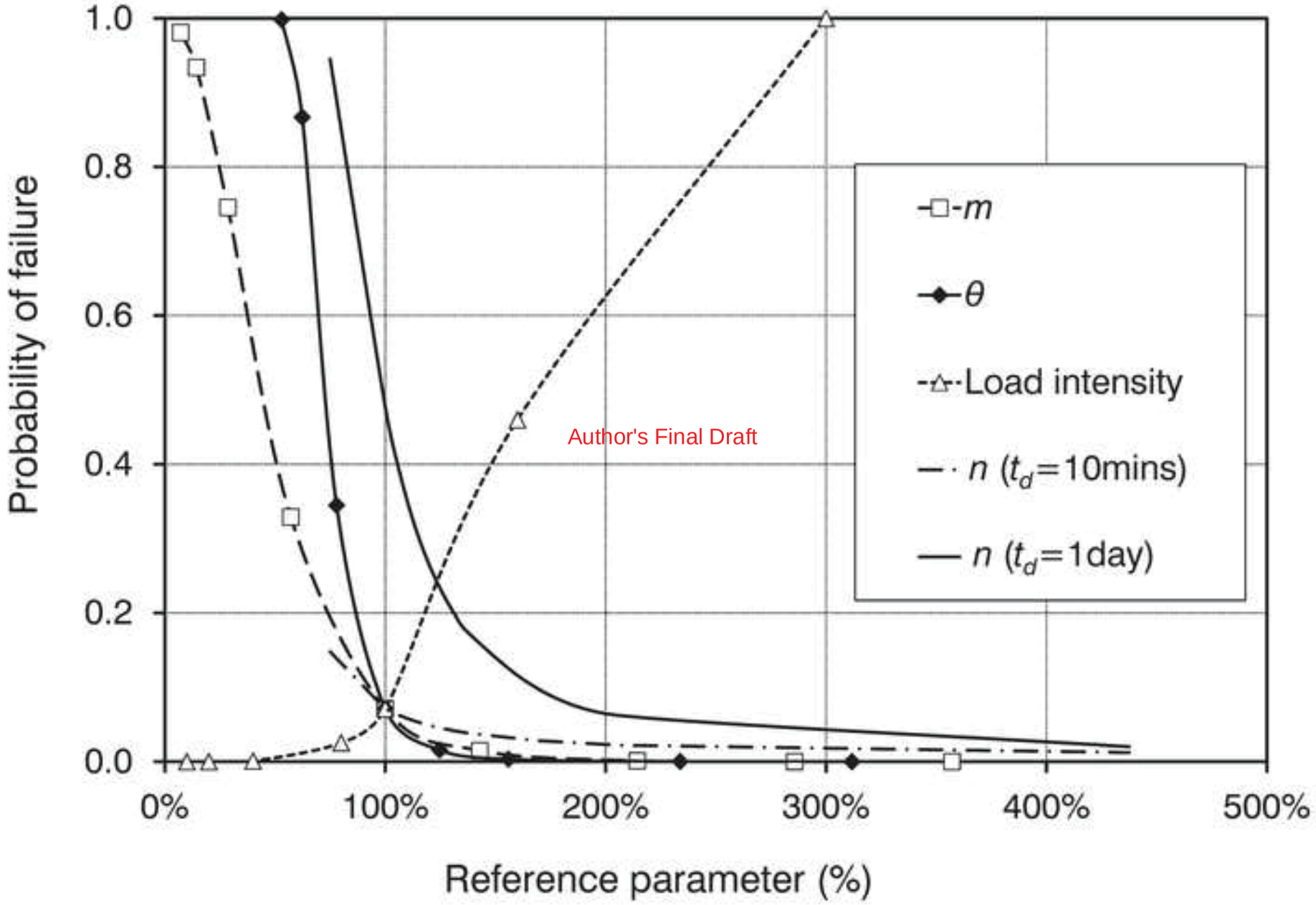

Figure 11

Click here to download high resolution image

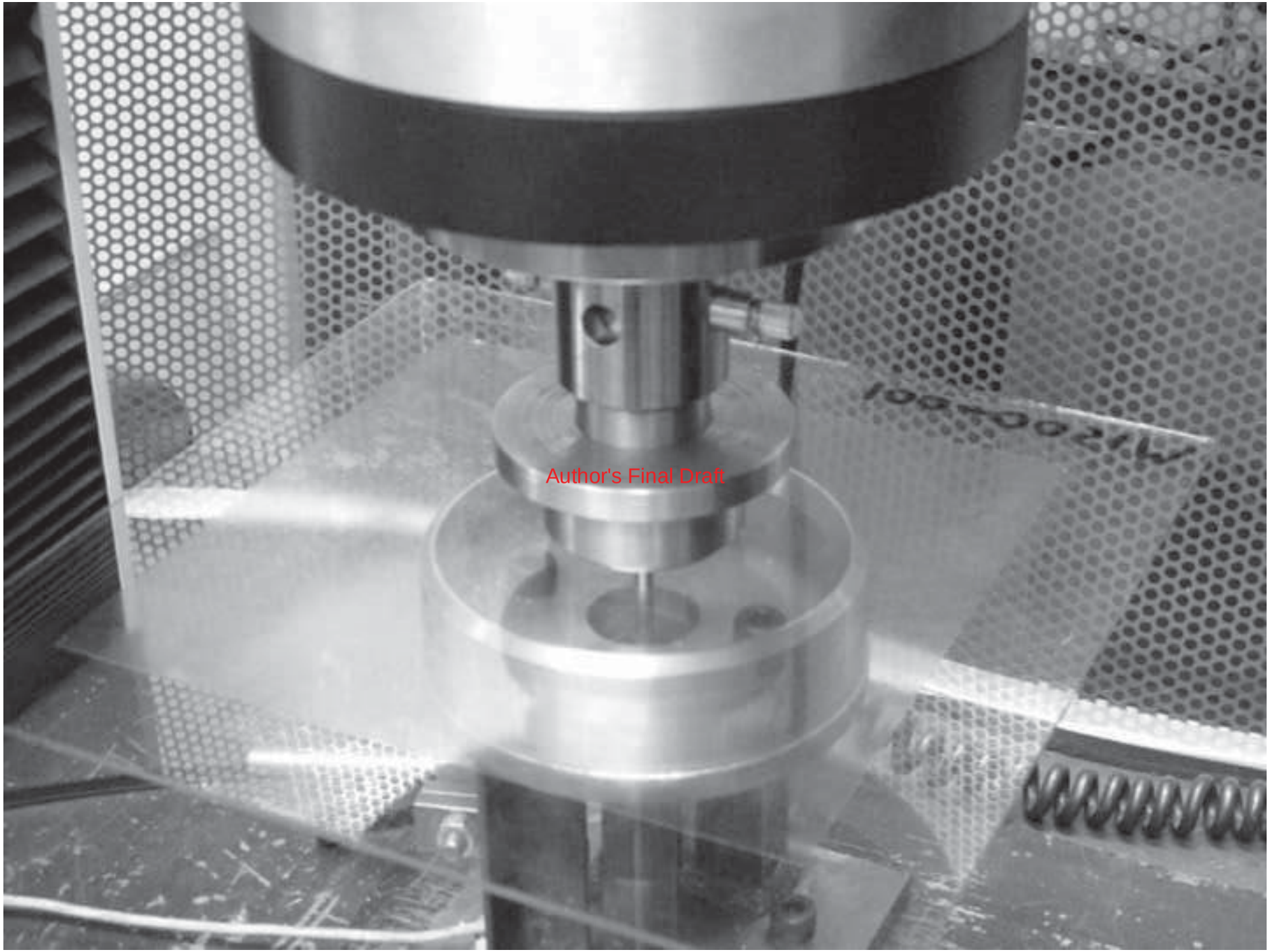

Figure 12
Click here to download high resolution image

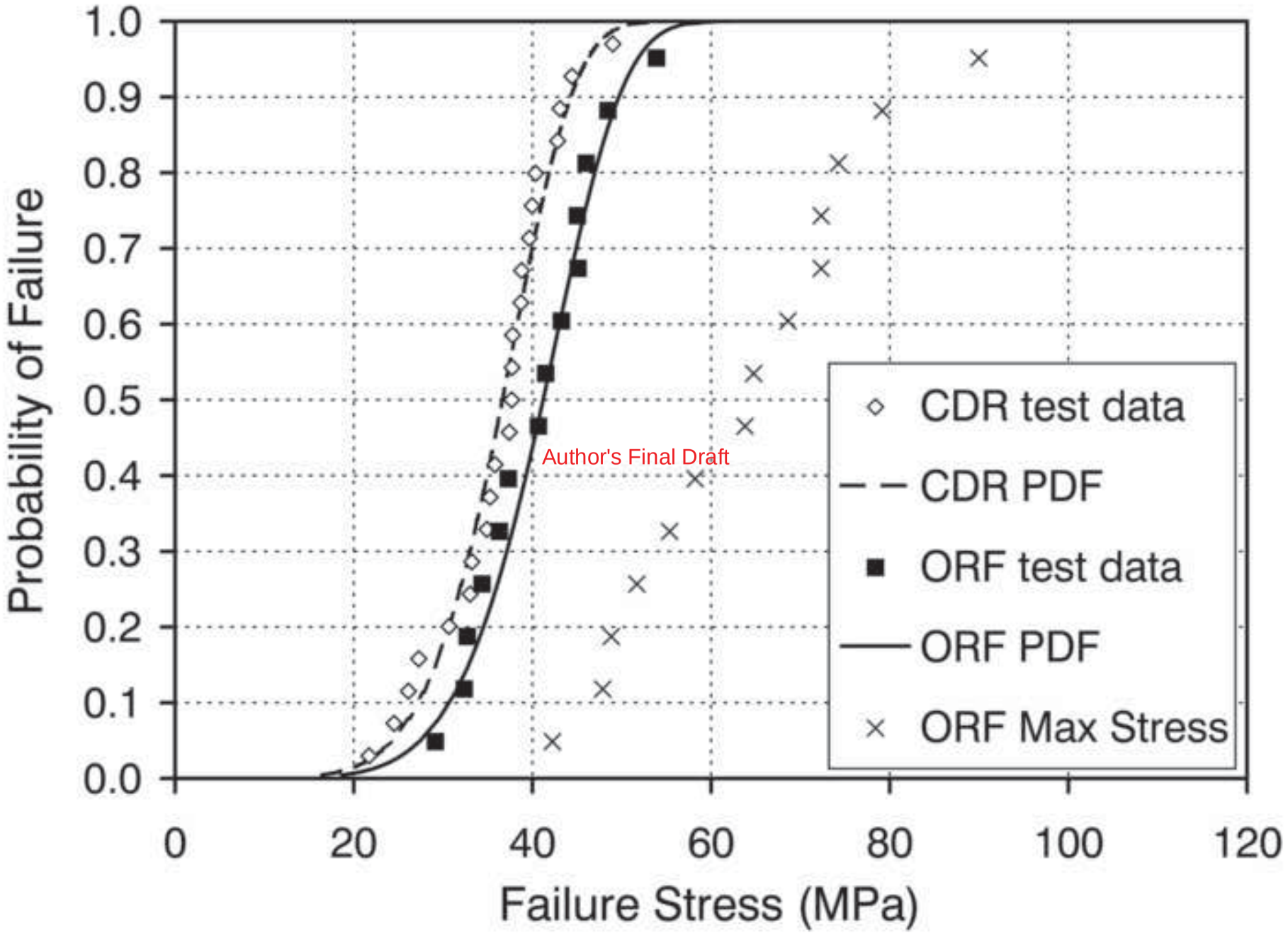

Figure A1
Click here to download high resolution image

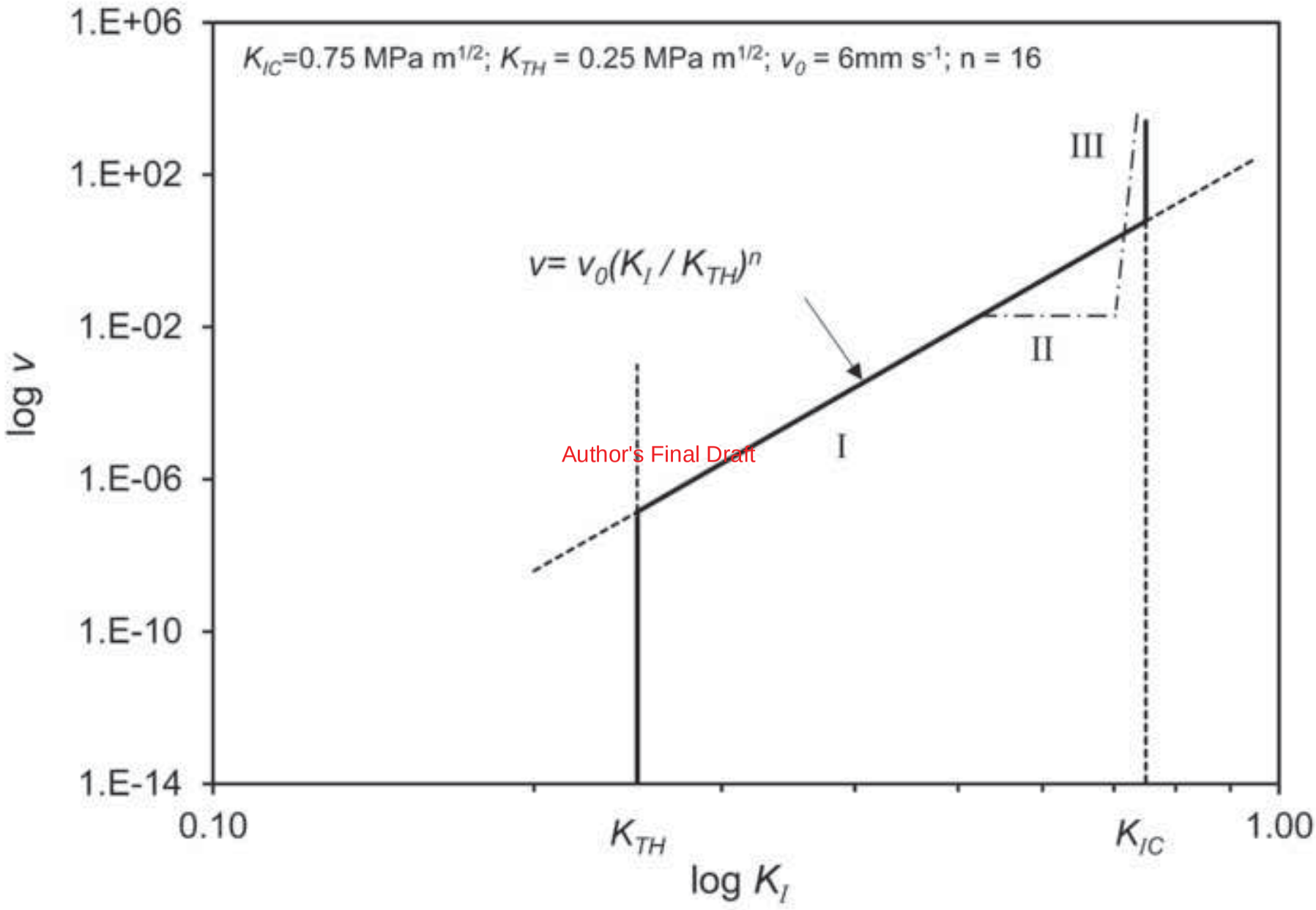

Figure A2
Click here to download high resolution image